On a New Heavy Resonance Search in Dilepton and Diphoton Channels at the LHC

A. Pankov[*], *A. Tsytrinov*

The Abdus Salam ICTP Affiliated Centre, GSTU, 246746, Gomel, Belarus

V. Bednyakov, N. Rusakovich

DLNP, JINR, 141980, Dubna, Russia

Abstract

Many models of physics beyond the Standard Electroweak Theory predict the existence of very heavy resonances that can manifest themselves as peaks or bumps in the cross sections at the LHC. It is possible that heavy resonances would be discovered early in the Large Hadron Collider program. The next step would be to measure their properties (spin, mass, coupling constants etc.) to identify the underlying theory that gave rise to the resonances. In this case, the spin determination of a peak, requiring the angular analysis of the events, becomes crucial in order to identify the relevant nonstandard source. We discuss the identification reach of heavy bosons with spin-2 Randall-Sundrum graviton excitations, spin-1 extra neutral gauge bosons Z', and spin-0 scalar resonance in Drell-Yan dilepton and diphoton events at LHC.

1 Introduction

In the coming years, it is anticipated that the CERN Large Hadron Collider (LHC), a *pp* collider with centre of mass energy $\sqrt{s} = 14$ TeV, will reveal a new level of understanding of the fundamental interactions when it starts to explore the TeV energy regime. For a number of reasons, including the

[*]E-mail:pankov@ictp.it

quadratic sensitivity of the Higgs boson mass to radiative corrections, it is generally believed that the Standard Model (SM) is a low energy effective limit of a more fundamental theory and numerous extensions of the SM have been proposed. Many of these extensions predict the existence of new heavy s-channel resonances [1]. If a kinematically accessible, a heavy resonance is expected to be discovered very early in the LHC program. Once such an object is discovered, the immediate task would be to measure its properties and identify its origins.

A key ingredient in determining the nature of a new resonance is to measure it's spin, mass and couplings to fermions. However, the observation of a peak/resonance at some large mass $M = M_R$ may not be sufficient to identify its underlying nonstandard model, in the multitude of potential sources of such a signal. Indeed, in "confusion regions" of the parameters, different models can give the same M_R and same number of events under the peak. In that case, the test of the peak/resonance quantum numbers, in the first place of the spin, is needed to discriminate the models against each other in the confusion regions. Specifically, one defines for the individual nonstandard scenarios a *discovery reach* as the maximum value of M_R for peak observation over the SM background, and an *identification reach* as the maximum value of M_R for which the model can be unambiguously discriminated from the other competing ones as the source of the peak.

Particularly clean signals of heavy neutral resonances are expected in the inclusive reactions at the LHC:

$$p + p \to l^+l^- + X \quad (l = e, \mu) \quad \text{and} \quad p + p \to \gamma\gamma + X, \qquad (1)$$

where they can show up as peaks in the dilepton (and diphoton) invariant mass M. While the total resonant cross section determines the number of events, hence the discovery reaches on the considered models, the angular analysis of the events allows to discriminate the spin-hypotheses from each other, due to the (very) different characteristic angular distributions. In the next sections we discuss the identification of the spin-2, spin-1 and spin-0 hypotheses, modelled by the Randall-Sundrum model with one warped extra dimension, a set of Z' models, and the R-parity violating sneutrino exchange [1], respectively.

2 Integrated observables

The total cross section for a heavy resonance discovery in the events (1) at an invariant dilepton (or diphoton) mass $M = M_R$ (with $R = G, Z', \tilde{\nu}$ denoting graviton, Z' and sneutrino, respectively) is:

$$\sigma(pp \to R) \cdot \mathrm{BR}(R \to l^+l^-) = \int_{-z_{\mathrm{cut}}}^{z_{\mathrm{cut}}} \mathrm{d}z \int_{M_R-\Delta M/2}^{M_R+\Delta M/2} \mathrm{d}M \int_{y_{\mathrm{min}}}^{y_{\mathrm{max}}} \mathrm{d}y \frac{\mathrm{d}\sigma}{\mathrm{d}M\,\mathrm{d}y\,\mathrm{d}z}. \tag{2}$$

In Eq. (2), $z = \cos\theta_{\mathrm{cm}}$ and y are the lepton-quark (or photon-quark) angle in the dilepton (or diphoton) center-of-mass frame and the dilepton rapidity, respectively, and cuts on phase space due to detector acceptance are indicated. Furthermore, ΔM is an invariant mass bin around M_R. To evaluate the number N_S of resonant signal events, time-integrated luminosities of 100 and 10 fb^{-1} will be assumed, as well as 90% reconstruction efficiencies for both electrons and muons and 80% for photons. Typical experimental cuts are: $p_\perp > 20$ GeV and pseudorapidity $|\eta| < 2.5$ for both leptons; $p_\perp > 40$ GeV and $|\eta| < 2.4$ for photons. To evaluate Eq. (2), the parton subprocesses cross sections will be convoluted with the CTEQ6 parton distributions. Next-to-leading QCD effects can be accounted for by K-factors, and for simplicity of the presentation we here adopt a flat value $K = 1.3$ for all considered processes.

In practice, due to the completely symmetric pp initial state, the event-by-event determination of the sign of z may at the LHC be not fully unambiguous. This difficulty may be avoided by using as the basic observable for the angular analysis the z-evenly integrated center-edge angular asymmetry, defined as:

$$A_{\mathrm{CE}} = \frac{\sigma_{\mathrm{CE}}}{\sigma} \quad \text{with} \quad \sigma_{\mathrm{CE}} \equiv \left[\int_{-z^*}^{z^*} - \left(\int_{-z_{\mathrm{cut}}}^{-z^*} + \int_{z^*}^{z_{\mathrm{cut}}}\right)\right] \frac{\mathrm{d}\sigma}{\mathrm{d}z}\,\mathrm{d}z. \tag{3}$$

In Eq. (3), $0 < z^* < z_{\mathrm{cut}}$ defines the separation between the "center" and the "edge" angular regions and is *a priori* arbitrary, but the numerical analysis shows that it can be "optimized" to $z^* \simeq 0.5$. The additional advantage of using A_{CE} is that, as being a ratio of integrated cross sections, it should be much less sensitive to systematic uncertainties than the "absolute" distributions (examples are the K-factor uncertainties from different possible sets of parton distributions and from the choice of factorization vs renormalization mass scales).

3 Angular distributions

We list, for the nonstandard models of interest here, the basic features relevant to the angular analysis and the spin-identification.

3.1 RS model with extra dimension

The simplest version, originally proposed as a rationale for the gauge hierarchy problem $M_{\mathrm{EW}} \ll M_{\mathrm{Pl}}$, consists of one warped extra spatial coordinate y with exponential warp factor $\exp(-k\pi|y|)$ (with $k > 0$ the 5D curvature assumed of order M_{Pl}), and two three-dimensional branes placed at a compactification distance R_c in y. The SM fields are localized to the so-called TeV brane, while gravity originates on the other one, the so-called Planck brane, but is allowed to propagate in the full 5D space. The consequence of the chosen space-time geometry is that, in the reduction to four dimensions, a Planck-brane mass spectrum with characteristic scale of order $\bar{M}_{\mathrm{Pl}} = 1/\sqrt{8\pi G_{\mathrm{N}}} \simeq 2.4 \times 10^{15}$ GeV, is exponentially "warped" down to the TeV-brane, and the cut-off on the effective theory becomes there $\Lambda_\pi = \bar{M}_{\mathrm{Pl}} \exp(-k\pi R_c)$. For $kR_c \simeq 12$, Λ_π is of the TeV order and this opens up the appealing possibility of observing gravitational effects at the LHC energies. Notably, these signatures consist of a tower of spin-2 graviton excitations that can be exchanged in processes (1) and show up as narrow peaks in M with the specific mass spectrum $M_n = x_n k \exp(-k\pi R_c)$, of order $\Lambda_\pi \sim$ TeV (x_n are the roots of $J_1(x_n) = 0$), and couplings to SM particles of order $1/\Lambda_\pi$.

The model can be conveniently parametrized in terms of M_G, the mass of the lowest graviton excitation, and of the "universal" dimensionless coupling $c = k/\bar{M}_{\mathrm{Pl}}$. Theoretically, the expected "natural" ranges are $0.01 < c < 0.1$ and $\Lambda_\pi < 10$ TeV.

For dilepton production, in self-explaining notations and with ϵ_q^G, ϵ_g^G and ϵ_q^{SM} the fractions of G-events under the M_R-peak initiated by $q\bar{q}$, gg and the SM background, respectively, the z-even distributions needed in (3) can at the leading order be expressed, as:

$$\frac{\mathrm{d}\sigma^G}{\mathrm{d}z} = \frac{3}{8}(1+z^2)\sigma_q^{\mathrm{SM}} + \frac{5}{8}(1-3z^2+4z^4)\sigma_q^G + \frac{5}{8}(1-z^4)\sigma_g^G, \qquad (4)$$

and:

$$A_{\rm CE}^{G} = \epsilon_q^{\rm SM}\, A_{\rm CE}^{\rm SM} + \epsilon_q^{G}\left[2\, z^{*5} + \frac{5}{2}\, z^{*}(1 - z^{*2}) - 1\right] + \epsilon_g^{G}\left[\frac{1}{2}\, z^{*}(5 - z^{*4}) - 1\right]. \tag{5}$$

For the diphoton events, the leading order RS resonance exchange contributions to $q\bar{q} \to G \to \gamma\gamma$ and $gg \to G \to \gamma\gamma$ can analogously be written as:

$$\frac{{\rm d}\sigma^{G}}{{\rm d}z} = \frac{5}{8}(1 - z^4)\sigma_q^{G} + \frac{5}{32}(1 + 6z^2 + z^4)\sigma_g^{G}, \tag{6}$$

and

$$A_{\rm CE}^{G} = \epsilon_q^{G}\left[\frac{1}{2}z^{*}(5 - z^{*4}) - 1\right] + \epsilon_g^{G}\left[-1 + \frac{5}{8}z^{*} + \frac{5}{4}z^{*3} + \frac{1}{8}z^{*5}\right]. \tag{7}$$

3.2 Extra neutral gauge bosons

The spin-1 hypothesis is in process (1) realised by $q\bar{q}$ annihilation into lepton pairs through Z' intermediate states. Such bosons are generally predicted by electroweak models beyond the SM, based on extended gauge symmetries. Generally, Z' models depend on $M_{Z'}$ and on the left- and right-handed couplings to SM fermions. In the sequel, results will be given for a popular class of models for which the values of these couplings are fixed theoretically, so that only $M_{Z'}$ is a free parameter. These are the Z'_{χ}, Z'_{ψ}, Z'_{η}, $Z'_{\rm LR}$, $Z'_{\rm ALR}$ models, and the "sequential" $Z'_{\rm SSM}$ model with Z' couplings identical to the Z ones.

The z-even angular distributions for the partonic subprocesses $q\bar{q} \to Z' \to l^+l^-$ have the same form as the SM and, therefore, the resulting $A_{\rm CE}$ is the same for all Z' models:

$$\frac{{\rm d}\sigma^{Z'}}{{\rm d}z} = \frac{3}{8}(1 + z^2)[\sigma_q^{\rm SM} + \sigma_q^{Z'}]; \tag{8}$$

$$A_{\rm CE}^{Z'} \equiv A_{\rm CE}^{\rm SM} = \frac{1}{2}z^{*}(z^{*2} + 3) - 1. \tag{9}$$

Consequently, the $A_{\rm CE}$-based angular analysis should have a considerable degree of Z' model independence.

3.3 R-parity violating sneutrino

R-parity is defined as $R_p = (-1)^{(2S+3B+L)}$, and distinguishes particles from their superpartners. In scenarios where this symmetry can be violated, supersymmetric particles can be singly produced from ordinary matter. In the dilepton process (1) of interest here, a spin-0 sneutrino can be exchanged through the subprocess $d\bar{d} \to \tilde{\nu} \to l^+l^-$ and manifest itself as a peak at $M = M_{\tilde{\nu}}$ with a flat angular distribution:

$$\frac{d\sigma^{\tilde{\nu}}}{dz} = \frac{3}{8}(1+z^2)\sigma_q^{\rm SM} + \frac{1}{2}\sigma_q^{\tilde{\nu}}, \tag{10}$$

$$A_{\rm CE}^{\tilde{\nu}} = \epsilon_q^{\rm SM}\, A_{\rm CE}^{\rm SM} + \epsilon_q^{\tilde{\nu}}(2z^* - 1). \tag{11}$$

Results on higher QCD orders and supersymmetric QCD corrections available in the literature indicate the possibility of somewhat large K-factors. The cross section is proportional to the R-parity violating product $X = (\lambda')^2 B_l$ where B_l is the sneutrino leptonic branching ratio and λ' the relevant sneutrino coupling to the $d\bar{d}$ quarks. We may take for X, presently not really constrained for sneutrino masses of order 1 TeV or higher, the (rather generous) interval $10^{-5} < X < 10^{-1}$.

4 Spin-diagnosis with $A_{\rm CE}$

The nonstandard models briefly described in the previous section can mimic each other as sources of an observed peak in M, for values of the parameters included in so-called "confusion regions" (of course included in their respective experimental and/or theoretical discovery domains), where they can give same number of signal events N_S.

One can try to discriminate models from from one another by means of the angular distributions of the events, directly reflecting the different spins of the exchanged particles. We define a "distance" among models accordingly:

$$\Delta A_{\rm CE}^{Z'} = A_{\rm CE}^{G} - A_{\rm CE}^{Z'} \qquad \text{and} \qquad \Delta A_{\rm CE}^{\tilde{\nu}} = A_{\rm CE}^{G} - A_{\rm CE}^{\tilde{\nu}}. \tag{12}$$

To assess the domain in the (M_G, c) plane where the competitor spin-1 and spin-0 models giving the same N_S under the peak can be *excluded* by the starting RS graviton hypothesis, a simple-minded χ^2-like criterion can be applied, which compares the deviations (12) with the statistical uncertainty $\delta A_{\rm CE}^{G}$ pertinent to the RS model (systematic uncertainties can easily be included). We impose the two conditions

$$\chi^2 \equiv |\Delta A_{\rm CE}^{Z',\tilde{\nu}}/\delta A_{\rm CE}^{G}|^2 > \chi^2_{\rm CL}. \tag{13}$$

Eq. (13) shows the definition of χ^2, and $\chi^2_{\rm CL}$ specifies a desired exclusion confidence level (3.84 for 95% CL). This condition determines the minimum number of events, $N_S^{\rm min}$, needed to exclude the spin-1 and spin-0 hypotheses (hence to establish the graviton spin-2), and this in turn will determine the RS graviton *identification* domain in the (M_G, c) plane. Of course, an analogous procedure can be applied to the identification of Z' and $\tilde{\nu}$ exchanges against the two competing ones as sources of a peak in process (1). In the next section we review the results obtained for the three spin-identification analyses based on $A_{\rm CE}$.

4.1 Spin-2 identification

By imposing the conditions (13), one finds the minimum number of events $N_S^{\rm min}$ vs M_G (and with $0.01 < c < 0.1$), needed to exclude at 95% CL the spin-1 as well as the spin-0 hypotheses once the spin-2 one has been assumed to be "true".

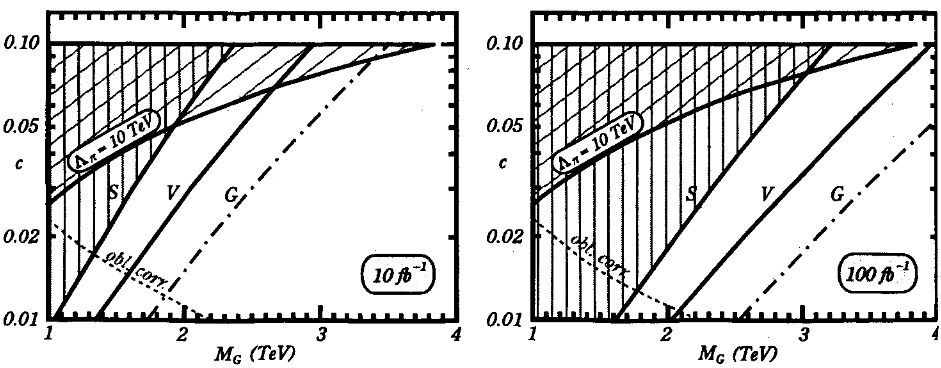

Figure 1. RS graviton discovery and identification from dilepton events.

Figure 1 shows the expected lowest lying graviton identification domain at 95% CL in the (M_G, c) plane from dilepton events ($l = e, \mu$ combined) at 14 TeV with time-integrated luminosities of 10 and 100 fb^{-1}. Basically, in

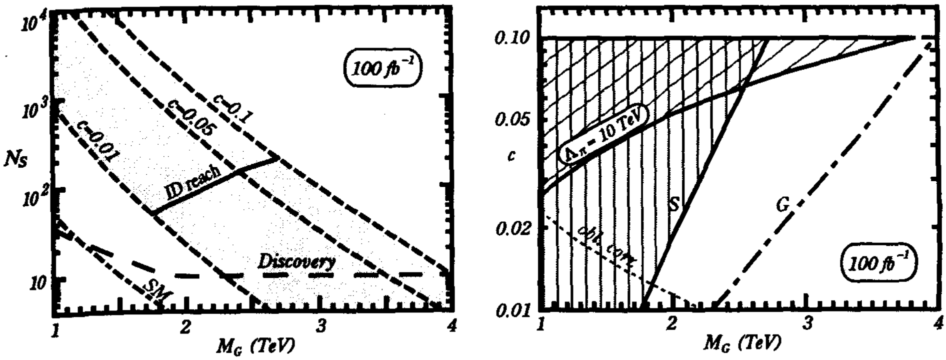

Figure 2. RS graviton discovery and identification from diphoton events.

this figure, the domain to the left of the line "G" is the discovery domain; that to the left of the "V" line is the exclusion domain of the Z' hypothesis; and that to the left of the "S" line represents the domain where the $\tilde{\nu}$ hypothesis (as well as the Z') can be excluded, hence the spin-2 identified. From the two panels of Fig. 1 one can read the expected graviton identification limits: $M_G < 1.1$ or 2.4 TeV for $c = 0.01$ or 0.1, respectively, at 10 fb^{-1}; $M_G < 1.6$ or 3.2 TeV for $c = 0.01$ or 0.1, respectively, at 100 fb^{-1}. The identification reach could therefore be a significant portion of the discovery domain, especially for the higher luminosity. On the other hand, the discovery domain is really constrained by the condition $\Lambda_\pi < 10$ TeV, if applied literally.

Figure 2 shows a preliminary attempt to assess the 95% CL identification reach on the RS spin-2 graviton excitation from the diphoton events in (1), by means of the $A_{\rm CE}$ analysis, for $\mathcal{L}_{\rm int} = 100$ fb^{-1} and cuts and photon reconstruction efficiencies as outlined in the Introduction. In this case, only a hypothetical spin-0 resonance decaying to two photons must be excluded. The left panel shows the $N_S^{\rm min}$ vs M_G for RS identification (or scalar hypothesis rejection) within $0.01 < c < 0.1$, while the right panel shows the identification domain in the (M_G, c) plane. This tentative example shows that diphoton events might have an identification sensitivity to the RS graviton comparable to the dilepton ones, with the spin-1 automatically excluded.

4.2 Spin-1 Z' identification

The $A_{\rm CE}$-based angular analysis can be applied quite similar to the preceding case, this time assuming that an observed peak in M is due to a Z', and evaluating the minimal number of events needed for excluding the spin-2 and spin-0 hypotheses. At the 100 fb^{-1} luminosity $N_S^{\rm min}$ turns out to be about 130 and 200 for exclusion of spin-2 and spin-0, respectively. This information can easily be turned into identification limits in terms of the relevant $M_{Z'}$. For the 14 TeV LHC nominal energy and luminosity 100 fb^{-1}, one could establish the Z' hypothesis (by exclusion of spin-2 and spin-0) for $M_{Z'} \leq 3.0 - 3.8$ TeV, depending on the particular model. In addition one can make pairwise comparisons (hence obtain identification) between the considered Z' models with same Z' mass on the basis of the different expected statistics, in the 1-2 TeV range for $M_{Z'}$.

4.3 Spin-0 sneutrino identification

As mentioned above the domain in the R-breaking parameter X allowed to sneutrinos can is so large that its discovery domain fully includes those of the RS resonance (with $0.01 < c < 0.1$) and of all Z's. The situation would be exactly the same even if we restricted X to the narrower interval 10^{-4}–10^{-2}.

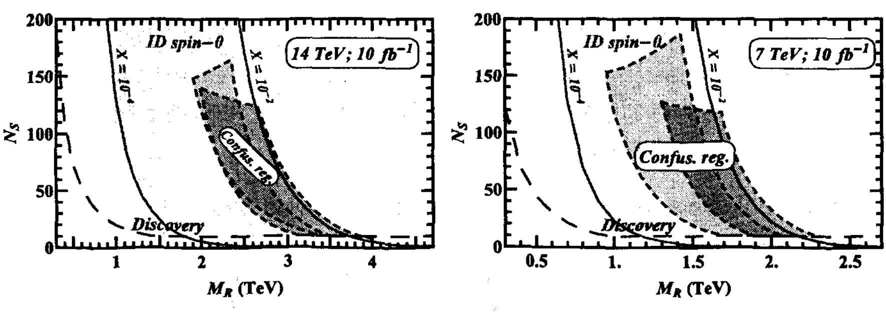

Figure 3. Sneutrino discovery and identification regions.

Figure 3 shows, as an example, the sneutrino confusion regions with RS and Z's vs $M_{\tilde\nu}$ for 10 fb^{-1}, with LHC energy 14 TeV (left panel) and 7 TeV (right panel), respectively. The Z' models are not all explicitly represented, the relevant curves lie in the domain between the rightmost (Z'_{ARL}) and the leftmost Z'_ψ dashed ones. The condition $\Lambda_\pi < 10$ TeV is not reported here. One can easily read off the minimal number of events vs $M_{\tilde{\nu}}$ needed for 95% CL exclusion of the RS resonance, of the spin-1 Z' hypotheses, and both, once a peak in dilepton events has been attributed to sneutrino exchange in (1). One finds that $N_S^{\rm min} \simeq 150$ events are needed for sneutrino identification via $A_{\rm CE}$, the relevant values of $M_{\tilde{\nu}}$ being constrained to the ranges 1.9–2.7 TeV and 1.1–1.7 TeV for LHC energies 14 TeV and 7 TeV, respectively. At 14 TeV and the highest luminosity $\mathcal{L}_{\rm int} = 100\ \mathrm{fb}^{-1}$, the range in $M_{\tilde{\nu}}$ would be 3.0–3.8 TeV.

Acknowledgements
This research has been partially supported by the Abdus Salam ICTP under the TRIL Programme and the Belarusian Republican Foundation for Fundamental Research.

References

[1] For details of the analysis and original references, see
I. A. Serenkova, A. A. Pankov, A. V. Tsytrinov and V. A. Bednyakov, Phys. Atom. Nucl. **73** (2010) 1266 [Yad. Fiz. **73** (2010) 1307];
P. Osland, A. A. Pankov, N. Paver and A. V. Tsytrinov, Phys. Rev. D **78**, (2008) 035008; **D79** (2009) 115021; **D82** (2010) 115017.